3582 Vol. 58, No. 13 / 1 May 2019 / Applied Optics Research Article

applied optics

Analysis and correction of stray thermal radiation in infrared optical systems including an experimental case study

ZHI-HUI YANG,[1,*] YONG-HUI MA,[1] JU-GUANG GUO,[1] WEI-WEI JIANG,[1] AND AI-HUI GENG[2]

[1]Science and Technology on Optical Radiation Laboratory, Beijing 100854, China
[2]Changchun Institute of Optics, Fine Mechanics and Physics, Chinese Academy of Sciences, Changchun 130033, China
*Corresponding author: textyangzhihui@126.com

Received 17 January 2019; revised 6 April 2019; accepted 9 April 2019; posted 10 April 2019 (Doc. ID 358007); published 30 April 2019

In infrared systems, the stray radiation from optical elements and mechanical structures is an important factor affecting quantitative measurements because the irradiance on detectors due to stray radiation depends on the operating temperature of the optical system. Without correcting for this effect, the accuracy of quantitative measurements made with such systems is degraded. To better understand this phenomenon, we derive herein a mathematical model that describes stray radiation as a function of temperature and use the model to quantitatively analyze the stray radiation of an infrared system at different operating temperatures. To test the theory, we use it to calculate the stray radiation from an experimental infrared system comprising a Cassegrain reflector in the first stage and a transmission mirror in the second stage. The maximum relative error between theory and experiment was 8.72%. At the same time, a corrective measure of stray radiation is provided to account for the effect of stray radiation on quantitative measurements. The relative error of quantitative measurements decreases from 2.16% to 0.31%. The measurement accuracy of the infrared system has been improved effectively.

https://doi.org/10.1364/AO.58.003582

1. INTRODUCTION

"Stray light" is the general term for all abnormal radiation in an optical system. Four main types of stray-light sources are possible in an optical system. The first type is external stray light, which comes from strong external light sources, such as the sun or the moon, and is reflected or scattered into the pupil of the optical system and then transmitted to the detector. The second type is stray light from a bright background in the field of view, and this type of stray light cannot be avoided in optical systems. The third type is stray light from multiple reflections and scattering of the target light in the field of view as it passes through the optical elements on its way to the detector. The fourth category is the stray light generated by thermal radiation from the infrared optical system itself, which is called internal stray radiation. The first type of stray light produces bright spots on the image, which are usually suppressed by the shades and shield rings. The second type of stray light is usually eliminated in the signal-processing stage. The third type of stray light forms "ghost images" on the image plane and may be reduced by applying antireflection coatings on the lens surface and by using an appropriate optical design. The fourth type of stray light affects the accuracy of quantitative measurements made by infrared optical systems and therefore must be eliminated [1–4].

In order to reduce the influence of stray light on optical system imaging and measurement, a series of in-depth studies have been carried out. Breault studied stray light transmitting theory and led the development of stray light analysis software ASAP [5]. Sheng and Mangzuo gave the test method of stray light evaluation index point source transmission (PST) for optical systems and established a device for PST testing [6]. Hahlweg and Rothe used a hemispheric spectroradiometer to measure the bi-directional reflectance distribution function of the material surface in the visible and near-infrared bands [7]. Pompeaa *et al.* studied the stray light suppression method of a ground-based astronomical telescope system and guided the structure design by stray light analysis [8]. Montanaro *et al.* studied stray radiation of the thermal Infrared sensor in Landsat 8 and proposed the correction method [9]. Shuai analyzed stray radiation of optical elements and mechanical structures in a Cassegrain infrared optical system and proposed a thermal control design [10]. However, at present, the research on stray light in optical systems mainly focuses on the influence of stray light on imaging and the measures to suppress stray light.

To make measurements with infrared radiation, an infrared optical system must first be accurately calibrated. However, the operating environment of such systems is complex and changeable, and the innumerable working conditions cannot all be simulated. Even if the optical system is calibrated prior to experimentation, the operating temperature, which directly affects the stray radiation in the system, changes over time, which changes the irradiance impinging on the detector. If the calibration data are obtained at an operating temperature that differs from the actual temperature, then an error will be introduced into measurements made with infrared radiation. Therefore, stray radiation must be analyzed as a function of operating temperature to determine how stray radiation affects measurements made with infrared radiation [11,12].

In this paper, a stray-radiation model based on operating temperature is established. The stray radiation of an infrared system at different operating temperatures is analyzed quantitatively. The accuracy of stray radiation analysis is verified by experiments. With correction for stray radiation in the calibration and measurement processes, the accuracy of measurements made with infrared radiation is guaranteed.

2. MATHEMATICAL MODEL

A. Stray-Radiation Model Based on Operating Temperature

The stray radiation received by the detector of an infrared optical system is mainly composed of radiation from the surface of optical elements and from the surface of the mechanical structures of the optical system. Because infrared measurement systems are mainly used to image distant targets, images of optical elements and of the mechanical structure take the form of defocused spots. In addition, infrared radiation from each microfacet on the surface of the mechanical structure can fully fill the detector over a certain stereo angle and thereby form a uniform radiation background.

As shown in Fig. 1, we consider as an object the surface of a source of stray radiation with radiance L. The optical lens group between the object and the detector is considered as a new imaging optical system, and the detector is considered as an aperture. The position and size of the pupil in the imaging optical system can be calculated by using geometrical optics: the position of the pupil center is set to $q(0, ye, 0)$, and the pupil diameter is set to D.

The equation describing the surface of the radiation source is $F(x, y, z) = 0$. An arbitrary point $p(x, y, z)$ is selected on the radiation surface, and a differential plane dS is selected near the point. The pupil surface is divided into many small area elements. The angle between the y axis and the connecting line of point $p(x, y, z)$ and the area element center is i. The angle between the z axis and the connecting line of point $q(0, ye, 0)$ and the area element center is φ. di and $d\varphi$ are differential variables of i and φ. The normal unit vector for the radiation surface at point $p(x, y, z)$ is $\vec{N}(\alpha_N, \beta_N, \gamma_N)$, whose arguments are

$$\alpha_N = F'_x/\Delta_N, \beta_N = F'_y/\Delta_N, \gamma_N = F'_z/\Delta_N, \tag{1}$$

where

$$\Delta_N = [(F'_x)^2 + (F'_y)^2 + (F'_z)^2]^{1/2}. \tag{2}$$

The unit vector $\vec{A}(\alpha, \beta, \gamma)$ of the principal ray that passes through the pupil center $q(0, ye, 0)$ from the point $p(x, y, z)$ is

$$\alpha = -x/\Delta_A, \beta = (y_e - y)/\Delta_A, \gamma = -z/\Delta_A, \tag{3}$$

where

$$\Delta_A = [x^2 + (y - y_e)^2 + z^2]^{1/2}. \tag{4}$$

The cosine of the angle ψ between the principal ray and normal line of the radiation surface at point $p(x, y, z)$ is

$$\cos\psi = \frac{\vec{A} \bullet \vec{N}}{|\vec{A}||\vec{N}|} = \alpha\alpha_N + \beta\beta_N + \gamma\gamma_N. \tag{5}$$

According to the definition of a solid angle, the solid angle ω subtended by the area element of the pupil with respect to point $p(x, y, z)$ is

$$\omega = \iint \sin i\,di\,d\varphi. \tag{6}$$

Then the radiation energy coming from the radiation surface that is received by the detector is

$$\Phi = \int L\cos(i - \psi)\mathrm{d}S\mathrm{d}\omega = L\int(\cos i \cos\psi + \sin i \sin\psi)\sin i\,\mathrm{d}i\mathrm{d}\varphi\mathrm{d}S. \tag{7}$$

Let the transmittance of the optical system from the stray-radiation source to the detector be τ_s, and let the area of the radiation detector be A_d; then the irradiance by stray radiation on the detector is

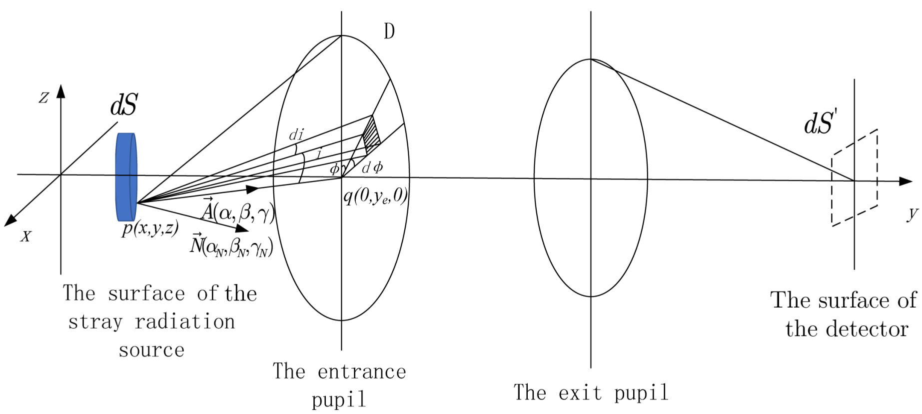

Fig. 1. Schematic diagram of the surface for analyzing stray radiation.

$$E = \Phi\tau_s \frac{1}{A_d} + \sigma = \frac{L\tau_s}{A_d}\int (\cos i \cos \psi + \sin i \sin \psi) \sin i \mathrm{d}i \mathrm{d}\varphi \mathrm{d}S + \sigma, \tag{8}$$

where σ is the dimensionless irradiance on the detector's target plane coming from the radiation of the optical elements and from the surfaces of the mechanical structure through multiple reflections and scatterings.

Once the opto-mechanical structure and related parameters of the infrared measuring system are determined, part of the expression for the opto-mechanical structure and the surface properties can be regarded as constant, which we call C. Thus, Eq. (8) can be written as [13,14]

$$E = \frac{LC}{A_d} + \sigma = \frac{1}{A_d}\int_{\lambda_1}^{\lambda_2} \frac{c_1}{\pi\lambda^5} \frac{1}{e^{c_2/(\lambda T)} - 1} \mathrm{d}\lambda \varepsilon C + \sigma. \tag{9}$$

Equation (9) shows that, once the detection wave band is determined, the variation in irradiance due to stray radiation on the detector depends only on the emissivity of the material surface and on the operating temperature of the system. Once the emissivity of the material surface is determined, this irradiance depends only on the operating temperature of the system.

B. Error Correction Model for Quantitative Measurement

In this work we use the concept of equivalent radiance to describe stray radiation energy, which means that the radiance of the standard blackbody-radiation source on the condition that the irradiance on the detector's target plane due to stray radiation is the same as that resulting from a standard blackbody-radiation source placed at the entrance pupil.

Assume that the irradiance on the detector's target plane due to all stray radiation is E_c; the equivalent radiance of the total stray radiation at the entrance pupil of the infrared system is then [15,16]

$$L_c = E_c \frac{F^2}{A_e \tau}, \tag{10}$$

where F and τ are the focal length and transmissivity of the infrared system, respectively; A_e is the area of the entrance pupil.

Before the infrared system may be used to make quantitative measurements, it must be calibrated. According to the theory of infrared-radiation calibration, the calibration curve in the linear region is given by [17,18]

$$\mathrm{DN} = kL + b, \tag{11}$$

where L is the equivalent radiance at the entrance pupil of the system being calibrated and DN is the response of the system. The constants k and b are the degree of calibration response and the background, respectively. The degree of calibration response k reflects the system's capacity to transmit radiation and the capacity of the detector to convert the optical signal into an electrical signal. The background b is the response of the detector to its voltage bias. The radiance L has two parts: the radiance L_s of a blackbody-radiation source at the pupil and the equivalent radiance L_c of stray radiation at the pupil from the system being calibrated. Thus,

$$\mathrm{DN} = k(L_s + L_c) + b. \tag{12}$$

When measuring the characteristics of the target radiation, the equivalent radiance of the stray radiation at the pupil of the infrared measurement system is L_c'. Thus,

$$\mathrm{DN}' = k(L_s + L_c') + b. \tag{13}$$

By comparing Eq. (12) with Eq. (13), we see that the use of the laboratory calibration data and the DN measured under a different operating temperatures to calculate the radiance of the target would produce errors of size

$$\Delta L = |L_c - L_c'|. \tag{14}$$

To avoid the error due to the quantitative analysis of the target's radiation characteristics, we make the following correction: First, we quantitatively analyze the equivalent radiance L_c at the entrance pupil caused by the stray radiation of the system being calibrated. We place low- and high-temperature blackbody-radiation sources at the pupil of the infrared system in turn and record the radiance of the blackbody and the response value of the detector. The degree of calibration response k and the background b can be determined by using

$$\begin{cases} \mathrm{DN}_1 = k(L_{s1} + L_c) + b, \\ \mathrm{DN}_2 = k(L_{s2} + L_c) + b, \end{cases} \tag{15}$$

where L_{s1} is the radiance of the low-temperature blackbody at the pupil, and DN_1 is the corresponding response value; L_{s2} is the radiance of the high-temperature blackbody at the pupil, and DN_2 is the corresponding response value.

Next, we quantitatively analyze the equivalent radiance L_c' at the entrance pupil due to the stray radiation of the system used to measure the target's radiation, which gives DN for the actual measurement. Finally, the actual radiance of the target L_s can be obtained by using [19,20]

$$L_s = \frac{\mathrm{DN}' - kL_c' - b}{k}. \tag{16}$$

3. SIMULATION AND EXPERIMENT

A. Simulation of Stray Radiation

A typical infrared measurement system uses a Cassegrain reflector system as the first stage and a transmission mirror group as the second stage. The infrared thermal imager receives parallel light rays from the transmission mirror group to the image and quantitatively measures the target's radiation. The main parameters are the aperture $D = 600$ mm, the system focal length $F = 1200$ mm, the diagonal view $2\omega = 0.435°$, and the detection band of 8–9 μm. Figure 2 shows the theoretical model. The main sources of stray radiation are the optical elements, such as the primary mirror, secondary mirror, dichroic mirror, compensating mirror, and focusing lens, and the mechanical structures, such as the support frames for the secondary mirror, the dichroic mirror, and the compensating mirror.

The infrared optical system is sensitive to thermal radiation. When mirror surfaces are in the light path, radiation from these surfaces travels through the optical system and reaches the detector. In contrast, radiation from the mechanical structure reaches the detector via reflection or scattering. Figure 3 shows the distribution of irradiance on the detector's target plane; this radiation is from the primary mirror at an operating

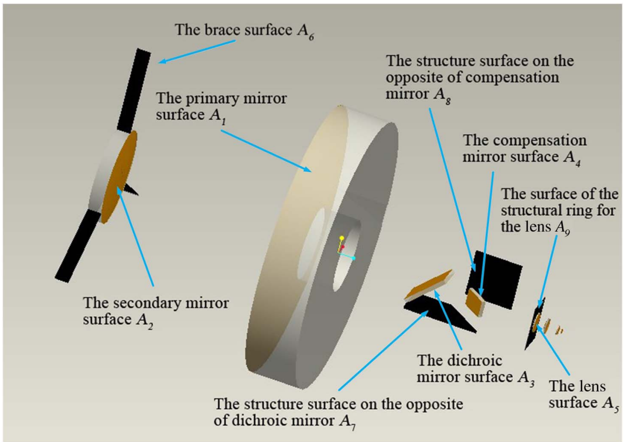

Fig. 2. Theoretical model of infrared optical system and stray-radiation source.

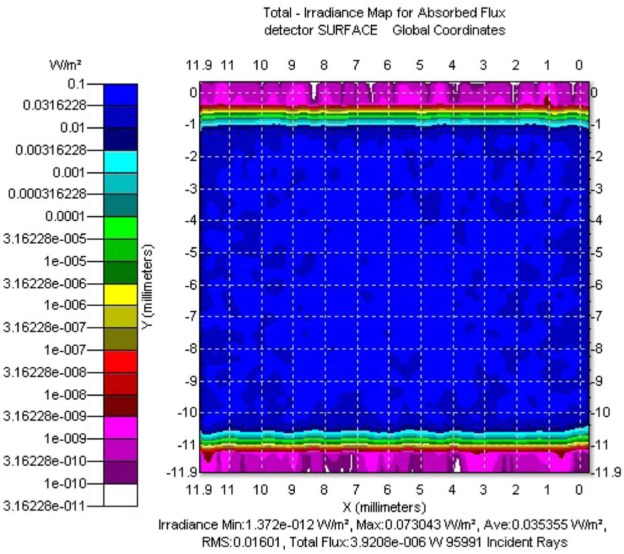

Fig. 3. Irradiance distribution on the detector target plane due to radiation from the primary mirror at an operating temperature of 300 K.

temperature of 300 K. Table 1 lists the irradiance statistics for the detector's target plane, where the radiation is from the surfaces of the optical elements and from the mechanical structures at various operating temperatures.

From the results of the analysis, we obtain the curve shown in Fig. 4, which gives the irradiance on the detector's target plane due to stray radiation as a function of operating temperature.

The results given in Table 1 show that the irradiance of the stray radiation of the infrared system increases gradually with increasing operating temperature. As the temperature increases from 220 to 320 K, the irradiance on the detector's target plane due to stray radiation increases by an order of magnitude. Figure 4 shows the irradiance due to stray radiation as a function of operating temperature.

B. Verification Experiment with Stray Radiation

To verify the validity of the quantitative analysis of stray radiation and the accuracy of its calculation, we measured the irradiance of the stray radiation. Here, we fully exploit the characteristics of the quantitative infrared thermal imager positioned at the back end of the infrared measurement system. Recall that, if a blackbody emitting radiance L_b fills the pupil, then the radiance detected by the thermal imager is also L_b. Figure 5 explains the situation in a schematic diagram of the experiment.

According to infrared radiometric calibration theory [21,22], the equivalent radiance of stray radiation at the entrance pupil of an infrared measurement system is

$$L_c = L_b \frac{A_b}{A_e} \frac{F^2}{F_b^2} \frac{\tau_b}{\tau} - L_s, \tag{17}$$

where L_b is the measured radiance of the system, A_b is the pupil area of the thermal imager, A_e is the pupil area of the system, F is the focal length of the system, F_b is the focal length of the thermal imager, τ is the transmittance of the system, τ_b is the transmittance of the thermal imager, and L_s is the radiance of a standard blackbody at the pupil of the system [23,24].

We thus positioned a standard blackbody-radiation source at the pupil of the infrared measurement system operated at various temperatures. The temperatures measured by the system were then converted to radiance. The equivalent radiance L_c due to stray radiation at the pupil entrance of the system can be calculated by using Eq. (17).

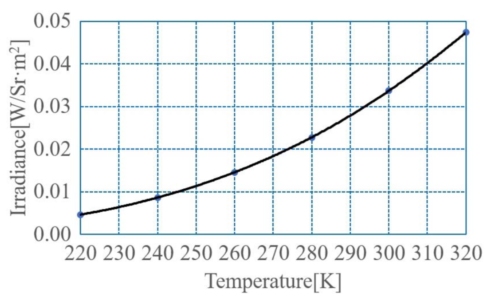

Fig. 4. Irradiance on the detector surface due to stray radiation as a function of operating temperature.

Table 1. Irradiance Due to Stray Radiation Impinging on the Detector Surface under Various Operating Temperatures

Operating Temperature [K]	220	240	260	280	300	320
From optical element [W/m²]	3.50×10^{-2}	6.48×10^{-2}	1.09×10^{-1}	1.71×10^{-1}	2.52×10^{-1}	3.55×10^{-1}
From mechanical structure [W/m²]	1.17×10^{-2}	2.17×10^{-2}	3.65×10^{-2}	5.73×10^{-2}	8.50×10^{-2}	1.19×10^{-1}
Total irradiance [W/m²]	4.67×10^{-3}	8.66×10^{-3}	1.46×10^{-2}	2.28×10^{-2}	3.37×10^{-2}	4.74×10^{-2}

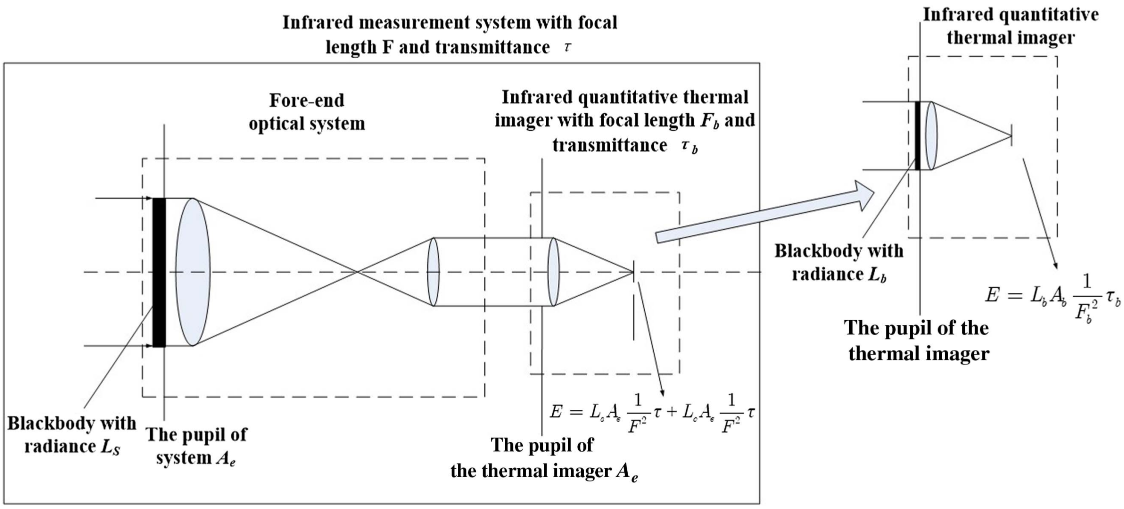

Fig. 5. Schematic diagram of validation experiment.

Table 2. Experimental Results of Stray Radiation Verification

Blackbody Temperature [K]	Environment Temperature [K]	Blackbody Radiance L_s [W/Sr · m^2]	Measured Display Temperature [K]	Measured Radiance L_b/[W/Sr · m^2]	Equivalent Radiance of Stray Radiation L_c [W/Sr · m^2]
278.15	267.15	5.92	268.45	4.90	1.38
283.15	265.15	6.59	272.75	5.41	1.47
293.15	265.15	8.09	280.45	6.41	1.49
313.15	264.15	11.71	296.95	8.98	1.42
333.15	264.15	16.24	311.65	11.76	1.40

Table 3. Theoretical Results and Experimental Measurement of Stray Radiation

Blackbody Temperature [K]	278.15	283.15	293.15	313.15	333.15
Equivalent radiance measured experimentally [W/Sr · m^2]	1.38	1.47	1.49	1.42	1.40
Equivalent radiance by theoretical analysis [W/Sr · m^2]	1.43	1.36	1.36	1.33	1.33
Relative error	3.60%	7.48%	8.72%	6.34%	5.00%

Table 2 lists the experimental results of measured stray radiation in the infrared measurement system.

At the same time, according to the actual operating temperature, the equivalent radiance of stray radiation from the infrared measurement system was analyzed and calculated theoretically. Finally, the errors of the equivalent radiance of stray radiation between the theoretical analysis and experimental measurement under the same working environment are obtained as shown in Table 3 and Fig. 6.

By comparing the experimental measurements with the theoretical results, we see that the stray radiation calculated theoretically is basically consistent with the experimental data. The maximum relative error is less than 8.72%. The experimental error is restricted to within a certain range, which verifies the accuracy of the theoretical calculation of stray radiation.

C. Revision Experiment of Quantitative Measurements

To simulate a long-distance target, a standard blackbody at 253.15 K was placed at the pupil of the infrared measurement system; it produced a radiance of 3.24 W/Sr · m^2. The calibration blackbody with different temperatures was placed at the pupil of the infrared measurement system, and the operating temperature was varied while recording the DN value

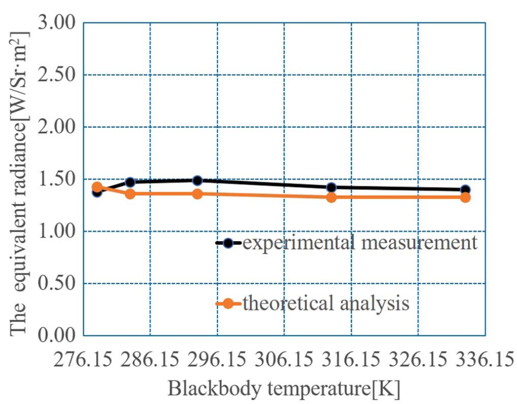

Fig. 6. Equivalent radiance due to stray radiation as a function of blackbody temperature. Radiance was calculated from theory and measured experimentally for each operating temperature.

Table 4. Experimental Results of Quantitative Measurement Revision

	Blackbody Temperature [K]	Blackbody Radiance $[\mathrm{W/Sr \cdot m^2}]$	Operating Temperature [K]	DN	Equivalent Radiance of Stray Radiation $[\mathrm{W/Sr \cdot m^2}]$
Equivalent target blackbody	253.15	3.24	265.15	2301	1.36
Calibration blackbody	293.15	8.09	267.15	3993	1.43
	303.15	9.79	267.15	4579	1.43

Table 5. Comparison of Radiance of Modified and Unmodified Equivalent Target Blackbody

	Actual Value of Equivalent Target Blackbody	Revised Calculated Value of Equivalent Target Blackbody	Unrevised Calculated Value of Equivalent Target Blackbody
Radiance/$(\mathrm{W/Sr \cdot m^2})$	3.24	3.23	3.17
Relative error	0%	0.31%	2.16%

for the infrared measurement system. Table 4 lists the results of these experiments.

According to Eq. (16), the calibration response k and the background b of the infrared measurement system can be obtained from the radiance and DN for the calibrated blackbody and the equivalent radiance due to stray radiation calculated from the operating temperature. The result is $k = 343.90$ and $b = 721.62$. According to Eq. (17), the revised equivalent target blackbody radiance can be calculated from DN for the equivalent target blackbody and the stray radiance calculated from the operating temperature at that time. The result is $3.23\ \mathrm{W/Sr \cdot m^2}$. In addition, by using Eq. (12), the radiance of the equivalent target blackbody without correction for stray radiation can be calculated from the experimental data of the calibration blackbody. The result is $3.17\ \mathrm{W/Sr \cdot m^2}$. Table 5 compares the radiance of the modified and unmodified equivalent target blackbodies.

Based on this comparison, we conclude that the modified calculated radiance of the equivalent target blackbody is closer to the actual value. The relative error decreases from 2.16% to 0.31%. Thus, we have improved the accuracy of quantitative measurements made with this infrared system.

4. CONCLUSION

We derive a theory of stray radiation based on the operating temperature of an infrared optical system. From a quantitative analysis, we obtain the irradiance at the detector's target plane due to stray radiation from the infrared optical system at various operating temperatures, and we determine how operating temperature affects the stray radiation from such a system. Furthermore, we analyze how stray radiation affects measurements made by the infrared system as a function of operating temperature and propose a method to correct for stray radiation, thereby improving the accuracy of quantitative measurements made with such systems.

REFERENCES

1. J. Niu, R. Zhou, Z. Liu, J. Yang, Z. Cai, and F. Lin, "Analysis of stray light caused by thermal radiation of infrared detection system," Opt. Tech. **32**, 73–79 (2006).
2. J. E. Hubbs, L. D. Brooks, and M. J. Nofziger, "Bidirectional reflectance distribution function of the infrared background signature survey (IBSS) telescope," Proc. SPIE **2260**, 128–139 (1994).
3. G. Wang, F. Xing, M. Wei, and Z. You, "Rapid optimization method of the strong stray light elimination for extremely weak light signal detection," Opt. Express **25**, 26175–26185 (2017).
4. G. H. Hunt and G. B. Shelton, "Experimental measurement and computer analysis of stray radiation in a telescope," Proc. SPIE **107**, 41–47 (1977).
5. R. P. Breault, "Problems and techniques in stray radiation suppression," Proc. SPIE **107**, 2–23 (1977).
6. L. Sheng and S. Mangzuo, "Study and test of stray light PST in infrared optical system," J. Infrared Millimeter Waves **15**, 375–378 (1996).
7. C. Hahlweg and H. Rothe, "Design of a semi-hemispherical spectroradiometer for fast acquisition of BRDF libraries in VIS and NIR," Proc. SPIE **5546**, 37–47 (2004).
8. S. M. Pompeaa, R. N. Pfisterer, and J. S. Morganc, "A stray light analysis of the apache point observatory 3.5-meter telescope system," Proc. SPIE **4842**, 128–138 (2003).
9. M. Montanaro, A. Gerace, A. Lunsford, and D. Reuter, "Stray light artifacts in imagery from the Landsat 8 thermal infrared sensor," Remote Sens. **6**, 10435–10456 (2014).
10. S. Shuai, "Optical-mechanical-thermal integrated design of multi-band common-aperture infrared system," Chin. J. Sci. Instrum. **34**, 387–393 (2013).
11. J. Stauder, R. W. Espplin, and L. Zollinger, "Stray light analysis of the SABER telescope," Proc. SPIE **2553**, 264–270 (1995).
12. D. L. Skelton, "Applying the tool: stray light cross-checks of the James Webb space telescope," Proc. SPIE **7731**, 77313U (2010).
13. K. Scott Ellis, "Stray light characteristics of the large synoptic survey telescope (LSST)," Proc. SPIE **7427**, 742708 (2009).
14. Y. Xucang, *Optical Design* (Beijing Institute of Press, 1998), pp. 337–342.
15. S. S. Olivier, L. Seppala, and K. Gilmore, "Optical design of the LSST camera," Proc. SPIE **7018**, 70182G (2008).
16. P. A. Lightsey and Z. Wei, "James Webb space telescope observatory stray light performance," Proc. SPIE **6250**, 62650S (2006).
17. B. Cuerden, J. Sebag, and S. West, "LSST mirror thermal performance," Proc. SPIE **5495**, 189–203 (2004).
18. C. Yang and L. Cao, "Radiation calibration and error analysis for a large-aperture infrared opto-electronic system," Infrared Laser Eng. **40**, 1624–1628 (2011).
19. Z. Jianqi and F. Xiaoping, *Infrared Physics* (Xi'an Electronic Science &Technology University, 2004), pp. 57–74.
20. T. Jia and G. Xin, "Calibration method for infrared radiation characteristics measuring system of test ranges," Infrared Laser Eng. **10**, 266–270 (2006).

21. X. Nanrong and B. Nanhua, *Infrared Radiation and the Control of Missile* (National Defense Industry, 1997), pp. 216–218.
22. D. Burke, T. Axelrod, C. Claver, and J. Frank, "Calibrations of LSST camera and telescope systems," Proc. SPIE **6267**, 626715 (2006).
23. C. Nianzeng and Y. Dayuan, *Radiometry and Photometry* (Beijing Institute of Press, 1990), p. 2.
24. H. Qiang, N. Xinhua, and S. Xueming, "Stray radiation analysis caused by interior heat radiation in infrared optical system," Opt. Tech. **28**, 348–352 (2006).